

Light-Induced Dielectrophoresis for Characterizing the Electrical Behavior of Human Mesenchymal Stem Cells

Kiara L. Lacy¹, Samuel Salib¹, Mary Tran², Tunplin Tsai¹, Rominna Valentine¹, Herdeline Ann M. Ardoña^{1,2,3,4}, Tayloria N. G. Adams^{1,2,4}

¹ Department of Chemical and Biomolecular Engineering, Samueli School of Engineering, University of California, Irvine ² Department of Biomedical Engineering, Samueli School of Engineering, University of California, Irvine ³ Department of Chemistry, School of Physical Sciences, University of California, Irvine ⁴ Sue & Bill Gross Stem Cell Research Center, University of California, Irvine

Corresponding Author

Tayloria N. G. Adams

tayloria@uci.edu

Citation

Lacy, K.L., Salib, S., Tran, M., Tsai, T., Valentine, R., Ardoña, H.A.M., Adams, T.N.G. Light-Induced Dielectrophoresis for Characterizing the Electrical Behavior of Human Mesenchymal Stem Cells. *J. Vis. Exp.* (196), e64909, doi:10.3791/64909 (2023).

Date Published

June 16, 2023

DOI

10.3791/64909

URL

jove.com/video/64909

Abstract

Human mesenchymal stem cells (hMSCs) offer a patient-derived cell source for conducting mechanistic studies of diseases or for several therapeutic applications. Understanding hMSC properties, such as their electrical behavior at various maturation stages, has become more important in recent years. Dielectrophoresis (DEP) is a method that can manipulate cells in a nonuniform electric field, through which information can be obtained about the electrical properties of the cells, such as the cell membrane capacitance and permittivity. Traditional modes of DEP use metal electrodes, such as three-dimensional electrodes, to characterize the response of cells to DEP. In this paper, we present a microfluidic device built with a photoconductive layer capable of manipulating cells through light projections that act as *in situ* virtual electrodes with readily conformable geometries. A protocol is presented here that demonstrates this phenomenon, called light-induced DEP (LiDEP), for characterizing hMSCs. We show that LiDEP-induced cell responses, measured as cell velocities, can be optimized by varying parameters such as the input voltage, the wavelength ranges of the light projections, and the intensity of the light source. In the future, we envision that this platform could pave the way for technologies that are label-free and perform real-time characterization of heterogeneous populations of hMSCs or other stem cell lines.

Introduction

Human mesenchymal stem cells (hMSCs) are recognized for their immunosuppressive properties¹, which have led to their use in therapeutics for the treatment of a variety of diseases, such as type II diabetes², graft versus host

disease³, and liver disease⁴. hMSCs are heterogeneous, containing subpopulations of cells that differentiate into adipocytes, chondrocytes, and osteoblasts. hMSCs are derived from adipose tissue, umbilical cord tissue, and

bone marrow, and their differentiation potential depends on the tissue of origin and the cell culture process used⁵. For instance, according to a study by Sakaguchi et al., hMSCs derived from adipose tissue are more likely to differentiate into adipocytes, whereas hMSCs derived from bone marrow are more likely to differentiate into osteocytes⁶. However, the impact of the tissue origin of hMSCs on their differentiation potential is a phenomenon that still needs to be further understood. Additionally, the varied differentiation potentials of hMSCs contribute to their inherent heterogeneity and create challenges in applying hMSCs for therapeutics. As such, the characterization, as well as sorting, of heterogeneous stem cell lines is critical for developing the *in vitro* and clinical application of these cells. Flow cytometry, the gold standard technique for examining differences in cellular phenotypes, utilizes cell-surface antigens and fluorescent dyes to label target cells and characterize them based on light scattering or cell-specific fluorescence characteristics^{6,7,8}. The disadvantages of this method include the limited availability of cell-surface antigen biomarkers, the high cost of the equipment and operation, and the fact that the cell surface staining could potentially damage the cell membrane and affect therapeutic applications^{9,10,11}. Therefore, exploring new techniques for cell characterization without compromising the native state of the cellular membrane could benefit the clinical performance of stem cell therapeutics.

Dielectrophoresis (DEP), a method of cell characterization that does not use surface labels, is the focus of this current work. DEP is a label-free or non-staining method implemented on microfluidic platforms to characterize heterogeneous populations of cells based on their electrical properties. DEP uses an alternating current (AC) electric field in replacement of fluorescence staining (i.e., a label-

based method)⁷. The other advantages of using DEP-based microfluidic devices for cell characterization include the use of small volumes (microliters), quick analysis time, minimal cell sample preparation requirements, minimal risk of sample contamination, minimal waste production, and low cost^{12,13}. Another benefit of DEP is the real-time monitoring of cells^{14,15,16}. For DEP, cells in suspension are exposed to a nonuniform AC electric field created with electrodes, and they become polarized⁶. This polarization causes cell movement and allows cell manipulation based on the frequency and voltage of the applied AC electric field. By adjusting the frequency, typically between 5 kHz to 20 MHz, cells can be attracted to or repelled away from the electrodes, corresponding to positive and negative DEP behavior, respectively⁶.

There are multiple modes of DEP characterization, namely, traditional, field flow fractionation, and light-induced, as classified by their electrode configuration and/or operational strategy¹⁷. The 3DEP analyzer, a traditional mode of DEP, incorporates physical metal electrodes and monitors the cellular response to an AC electric field. This system uses a chip consisting of microwells with multiple three-dimensional circular electrodes and detects changes in light intensities to characterize cell DEP behavior^{18,19,20,21}. Positive DEP is observed as the cells moving toward the edges of the circular electrodes along the walls of the microwell, resulting in increased light intensity in the center of the microwell. Negative DEP is observed as cells clustering in the center of the microwell away from the circular electrodes, resulting in decreased light intensity in the center of the microwell. These two phenomena are represented in **Figure 1**. Traditional DEP methods have the capability to characterize the electrical properties of heterogeneous cell populations^{18,20,21}. For example, Mulhall et al. demonstrated the potential to

distinguish between normal oral keratinocytes (HOK) and malignant oral keratinocyte (H357) cell lines based on differences in membrane capacitance²¹ using the 3DEP analyzer. However, one limitation of traditional modes of DEP is the fixed electrode geometry. Since hMSCs are heterogeneous, it is advantageous to have the ability to easily modify the electrode geometries during DEP assessments. For instance, being able to modify the electrodes or electrode arrays in real-time for single-cell trapping allows for the cells to be characterized based on velocity and DEP behavior. The application of real-time electrode modification in DEP assessments of hMSCs allows for the single-cell analysis of hMSCs right after sourcing them from the sample tissue to characterize the heterogeneity of the sample population.

To overcome the limitation of traditional modes of DEP (i.e., fixed physical electrodes) and explore new opportunities for real-time electrode configuration modifications using the DEP phenomenon, light-induced DEP (LiDEP) has been explored. LiDEP is a non-traditional mode of DEP that manipulates cells using a photoconductive microfluidic device^{22,23} *via* light projections, localized electrodes create a nonuniform electric field, similar to the traditional DEP method. This approach also allows for flexibility in the electrode geometry and for moving the electrodes within the microfluidic device. This mitigates the limitation seen with fixed electrodes and provides the opportunity to gain more information about cellular heterogeneity. LiDEP has been used to detect and analyze different cell types in homogeneous and heterogeneous populations of cells^{22,23,24}. For example, Liao et al. used LiDEP to separate circulating tumor cells (CTCs) expressing the epithelial cell adhesion molecule (EpCAM^{neg}) from red blood cells to explore their significance in cancer metastasis²². Single-cell analysis with LiDEP has successfully been used to characterize and

manipulate cancer cells with the stratification of pancreatic tumorigenicity²³ and the analysis of CTCs in samples pre- and post-metastasis²⁴.

Here, we describe how LiDEP can be utilized to manipulate hMSCs with a variety of electrode geometries (circle, diamond, star, and parallel lines) and system settings (applied voltage, light intensity, and microfluidic device material), thus offering an approach to characterize the behavior of human-derived stem cells with virtual electrodes.

Protocol

1. LiDEP microfluidic device fabrication

NOTE: The fabrication process consists of combining three layered components: (i) a photoconductive layer with amorphous silicon (A:Si) and molybdenum deposited onto an indium tin oxide (ITO) glass substrate; (ii) a microchannel layer cut out from double-sided tape; and (iii) a top ITO glass substrate with holes drilled for the inlet and outlet of the cell suspension.

1. Glass coating of photoconductive indium tin oxide (ITO)
 1. Clean the ITO-coated glass substrate (15-20 Ω resistance) by flowing nitrogen (N_2) gas at the surface at a flow rate that is sufficient to move visible dust particles. After this step, rinse the substrate with acetone.
 2. Transfer the ITO-coated glass slide to an isopropyl alcohol bath to wash off the acetone residue, rinse with DI water, and flow N_2 gas again until the substrate is completely dry.
 3. Place the glass slide with the ITO-coated side up into the vacuum sputtering system.

4. Sputter a 10 nm thick layer of molybdenum onto the ITO-coated glass substrate (molybdenum target) with a deposition rate of 0.7 Å/s and a deposition time of 140 s.
 5. Add a shadow mask to one side of the glass substrate to leave 2 mm from the edge of the glass substrate uncovered for electrical connections. Deposit 1 μm of A:Si using inductively coupled plasma-plasma enhanced chemical vapor deposition (ICP-PECVD), as described in Medjdoub et al.²⁵.
 6. Clean the slide with N₂ gas to remove dust and other impurities. For any A:Si deposited under the shadow mask, submerge the edge up to the 2 mm mark in a 25% w/v potassium hydroxide solution to etch the A:Si.
2. LiDEP chip device fabrication
1. To form the microchannel, obtain double-sided tape (52 mm x 25 mm), and punch holes (diameter = 4 mm) 5-6 mm away from the edge of the shorter dimension and centered between the longer sides of the tape. Use a scalpel to cut two straight lines (3 mm apart) across the holes. Ensure the protective sheets on both faces of the double-sided tape are on during the entire microchannel cutting step.
 2. Drill two 3 mm diameter holes in the top ITO glass slide. The tape can be aligned on top of the ITO-coated glass, with the long edge of the tape aligning with the long edge of the glass. Mark the hole location with a washable marker. Make sure the drilled holes align with the holes punched in the double-sided tape. These two holes will act as the inlet and outlet holes of the microfluidic device.
 3. Remove one side of the protective film on the double-sided tape, align the holes in the tape and the top ITO glass slide, and press them together. Press gently to remove air pockets, especially near the microchannel. Air pockets may allow the medium or other solutions to seep under the tape, which can damage or cause mold in the microfluidic device.
 4. Remove the other protective film from the double-sided tape, and press onto the molybdenum and A:Si-coated ITO glass side. Match the edge of the photoconductive slide that is opposite to the 2 mm clearance side to the edge of the double-sided tape that is toward the center of the top ITO glass slide. There will be hangover from the top ITO glass slide and the photoconductive material-coated ITO glass slide.
 5. Press on a flat surface to ensure good adhesion. A schematic of the glass substrate and double-sided tape layers is illustrated in **Figure 1A**. Cut off excess tape on the side.
 6. Apply copper tape to the edges of layer A and layer C to connect the function generator. Do this by wrapping the tape on the side of the ITO or photoconductive material, depending on if it is layer A or layer C, from the edge of the double-sided tape to about 3 cm onto the uncoated side of the glass substrate.
 7. To ensure successful device fabrication, use a multimeter to test for a resistance reading between the coated slides of both glass substrates and the copper tape that was attached to the glass.
3. DEP buffer preparation

1. Measure out 4.25 g of sucrose, and place it into a 50 mL conical tube. Then, measure out 0.15 g of glucose, and place it into the same 50 mL conical tube.
 2. Fill the conical tube with 25 mL of ultrapure water, close the lid, and mix. Once about half of the sucrose and glucose have dissolved, fill the conical tube with ultrapure water up to the 50 mL line. Mix vigorously until all the sucrose and glucose are dissolved. DEP buffer solution contains 8.5% (w/v) sucrose and 0.3% (w/v) glucose.
 3. Obtain 20 mL of the prepared sucrose and glucose solution, and place it into a 50 mL conical tube. Then, measure out 0.1 g of bovine serum albumin (BSA), and place it into the 50 mL conical tube containing the sucrose and glucose solution. Vortex until the BSA is dissolved. The final DEP buffer solution contains 0.5% (w/v) BSA.
4. Cell preparation
1. Obtain at least 1×10^6 cells (hMSCs or HEK 293) suspended in 1 mL of growth medium using the cell culture protocol described in previous studies^{26,27}. Place the cell suspension into a 10 mL centrifuge tube.
 2. Centrifuge the HEK 293 cells at $201 \times g$ for 5 min and the hMSCs at $290 \times g$ for 10 min. After centrifugation, aspirate the supernatant, and resuspend the cells in 1 mL of the DEP buffer solution with 0.5% BSA. Be sure not to add the buffer solution too fast because bubbles may form.
 3. Repeat the centrifugation process two more times, and then resuspend the cells in the DEP buffer

with 0.5% BSA for LiDEP characterization. The cell preparation protocol listed is enough for 10 runs. For example, one frequency test requires at least 15 runs, and, thus, 2 mL of cells at a concentration of 1×10^6 cells/mL needs to be made.

2. LiDEP characterization

1. Experimental setup
 1. Assemble the following equipment for the experimental setup for quantifying the cellular responses to LiDEP: a laptop, a projector, an objective lens, a digital microscope, and a function generator. Use the laptop to design the light projections (star, diamond, three lines, and oval), and connect it to the projector.
 2. Use the projector as the light source to display the light projections onto the photoconductive surface (layer C) of the LiDEP chip. Set it up so that the light from the light source (projector) travels through a 10x objective lens onto the microchannel region of the LiDEP chip. The 10x objective lens sits on top of the projector lens. **Supplementary Figure 1** shows the integration of the projector into the LiDEP system.
 3. Connect the LiDEP chip to the function generator to apply the AC electric field. Observe the cells experiencing the LiDEP force by using the digital microscope for imaging and video recording. **Figure 1B** shows a schematic of the experimental apparatus. Follow standard cell culture protocols^{26,27} for all the cells tested.
2. Experimental procedures
 1. Flush the microchannel with 70% ethanol, followed by 0.5% BSA solution. Flush the microchannel again

- with 0.5% BSA solution two more times to ensure that the ethanol and previous cells are completely washed away. Cells that have already been exposed to the DEP field will respond differently than fresh cells and may disrupt the data collection.
2. Remove the 0.5% BSA solution with a pipette, and fit the microfluidic device into the device holder.
 3. Attach alligator clips to each of the copper tape connections on the device. Set the function generator to the desired voltage (voltage peak-to-peak, V_{pp}) and frequency (Hz). The frequency range tested here was 30 kHz to 20 MHz.
 4. Add 70 μL of cell suspension (cells + DEP buffer solution with 0.5% BSA) into the device microchannel. Due to the thinness of the microchannel (~ 0.05 mm), spillage out of the inlet and outlet holes may occur. To help reduce the amount of spillage, use a smaller pipette tip, and tilt the tip slightly in the hole toward the microchannel. Any access solution (0.5% BSA or cells in solution) can be wiped away with single-use paper wipes and discarded into biohazard waste.
 5. Project the desired virtual electrode geometry (here, circles, diamonds, stars, and/or parallel lines) onto the LiDEP chip.
 6. In the digital microscope software, set the video length to 3 min. Set a lab timer to 2 min 30 s. Once the cells are stationary in the microchannel of the LiDEP chip, press **Start** in the digital microscope software to begin the video recording process.
 7. Wait 10 s, then press the **ON** button of the function generator channel output to apply the AC electric field, and press **Start** for the timer. Monitor the cell

DEP behavior through the digital microscope, and prevent shaking or movement around the setup.

8. Once the timer goes off, press the **ON** button of the function generator channel output. This turns the function generator channel output off, and the AC electric field is no longer supplied through the electrodes. Stop the video recording at 3 min, and save to the digital microscope for future analysis.
9. Pipette the cells out of the outlet end of the LiDEP chip by slowly pushing 60 μL of DEP buffer with 0.5% BSA into the microchannel and simultaneously collecting at the outlet. Continue until there are little to no cells in the microchannel.
10. Repeat steps 2.2.3-2.2.9 until all frequencies have been tested.

Representative Results

Voltage and electrode color tests were completed using the procedure above with a slight variation in step 2.2.3 and step 2.2.10. For the voltage test, the electrode color and frequency remained constant, and 5 V_{pp} , 10 V_{pp} , and 20 V_{pp} were applied. For the electrode color test, the applied voltage and frequency were held constant at 30 kHz and 20 V_{pp} , and blue, red, white, and yellow (referenced by HEX color codes #4472C4, #FF0000, #FFFFFF, and #FFFF00, respectively) projected electrodes were examined. The cell viability was examined by staining the cells with trypan blue and counting the number of live and dead cells using a hemocytometer.

With the LiDEP setup, we were able to manipulate the hMSCs and generate DEP response curves in response to the input frequency, which is one way to characterize the electrical behavior of cells. A series of experiments were conducted to find the optimal operating conditions by manipulating

parameters such as the applied voltage and the projected electrode color (i.e., shapes with distinct colors created with a graphic editor software) to observe consistent cell behavior to the nonuniform AC electrical field generated with the virtual electrodes. The data collected for cell responses using LiDEP, non-traditional DEP, were compared to results from the 3DEP analyzer, traditional DEP.

The first optimization test focused on the positive DEP response of hMSCs (i.e., the cells moving toward the virtual electrode) in the LiDEP chip. The cells not exhibiting a positive DEP response either displayed a negative DEP response by moving away from the virtual electrode, were stationary and rotating, or were unresponsive to the electric field. The response of the cells was quantified by tracking their velocities ($\mu\text{m/s}$) in ImageJ during a 2 min 30 s period. A yellow oval projection was used for the virtual electrode, and the applied voltages of 5 V_{pp} , 10 V_{pp} , and 20 V_{pp} were examined at a set frequency of 30 kHz. We focused on cells that were within 50 μm of the virtual electrode while the AC electric field was on for consistency and to minimize outliers. The 20 V_{pp} resulted in the fastest cell movement of the HEK 293 cells, with an average velocity of 0.035 $\mu\text{m/s}$, and this was followed by 0.032 $\mu\text{m/s}$ at 10 V_{pp} and 0.020 $\mu\text{m/s}$ at 5 V_{pp} , meaning these cells represent a relatively homogeneous control. A similar trend was observed for hMSCs, which had an average velocity of 0.051 $\mu\text{m/s}$ at 20 V_{pp} , 0.036 $\mu\text{m/s}$ at 10 V_{pp} , and 0.025 $\mu\text{m/s}$ at 5 V_{pp} , as in **Figure 2A** (here, * indicates $p < 0.05$). At 20 V_{pp} , it was observed that the hMSCs experienced positive and negative DEP simultaneously. This was not observed at 10 V_{pp} and 5 V_{pp} . The viability findings of the hMSCs after experiencing the DEP force showed that higher voltages generally resulted in lower cell viability, with 66% of cells viable at 5 V_{pp} , 58% of the cells viable at 10 V_{pp} ,

and 57% of the cells viable at 20 V_{pp} , as in **Figure 2B** (here, ** indicates $p < 0.01$).

Due to LiDEP being an optical-based system, the light intensity and electrode color are parameters that can be easily tuned to control the performance of the LiDEP chip. Here, different electrode colors (white, yellow, red, and blue) generated based on the shape being projected were evaluated to determine the effect on the cells' DEP responses. HEK 293 cells and hMSCs were evaluated at 20 V_{pp} and 30 kHz. White-, yellow-, red-, and blue-colored electrodes were chosen, but the illumination through the LiDEP chip was affected by the photoconductive layer, which had a red-orange color. Thus, the projected white electrode appeared yellow with a white interior, the red electrode appeared orange with a red outline, and the blue electrode appeared light green (**Figure 3A-D**). The power outputs for these four colors were as follows: 77.7 $\mu\text{W} \pm 0.7 \mu\text{W}$, 92.7 $\mu\text{W} \pm 1.3 \mu\text{W}$, 21.9 $\mu\text{W} \pm 0.2 \mu\text{W}$, and 56.7 $\mu\text{W} \pm 0.9 \mu\text{W}$ for white, yellow, red, and blue, respectively. This strongly suggests that yellow and white had the strongest DEP field, while blue and red were weaker, as in **Figure 3E** (here, *** indicates $p < 0.001$ for HEK 293 cells and ** indicates $p < 0.01$ for hMSCs). Stationary rotation of the cells on the edges of the yellow and white virtual electrodes during the application of the DEP force was also observed. For all electrode color variations, simultaneous negative and positive DEP responses occurred, correlating to what was shown at 20 V_{pp} for the voltage test. Additionally, while the velocity of the cells varied based on the electrode color, almost all the cells within the 50 μm boundary responded to LiDEP. The size of the hMSCs was measured as 19.2 $\mu\text{m} \pm 5.8 \mu\text{m}$.

To assess the capability of LiDEP compared to DEP with conventional electrodes, we assessed the differences

between the DEP behavior of cells using LiDEP to that of cells analyzed by the 3DEP analyzer. The DEP response of hMSCs was measured in a low-conductivity DEP buffer solution with 0.5% BSA (~100 $\mu\text{S}/\text{cm}$). To mimic the 3DEP analyzer, a single oval yellow virtual electrode was projected at 10 V_{pp} . The DEP behavior of the hMSCs was characterized from 30 kHz to 20 MHz. At frequencies lower than 25 kHz, we observed electrolysis, which resulted in bubble generation at the surface of the metal layer within the microfluidic device. For LiDEP, at lower frequencies, the hMSCs experienced positive DEP force, as in **Figure 4A**,

represented as the percentage of cells attracted to the virtual electrode. The cells started with a strong positive DEP force, which weakened as the frequency increased. The cells experienced the strongest positive DEP force from 30 kHz to 97 kHz. After applying the AC electric field at these frequencies, some cells became unresponsive, while other cells showed negative DEP behavior. This trend deviates from the observed response quantified using the 3DEP analyzer; the cells increased in positive DEP from 37 kHz to 255 kHz and decreased in positive DEP from 1,772 kHz to 20 MHz, as in **Figure 4B**.

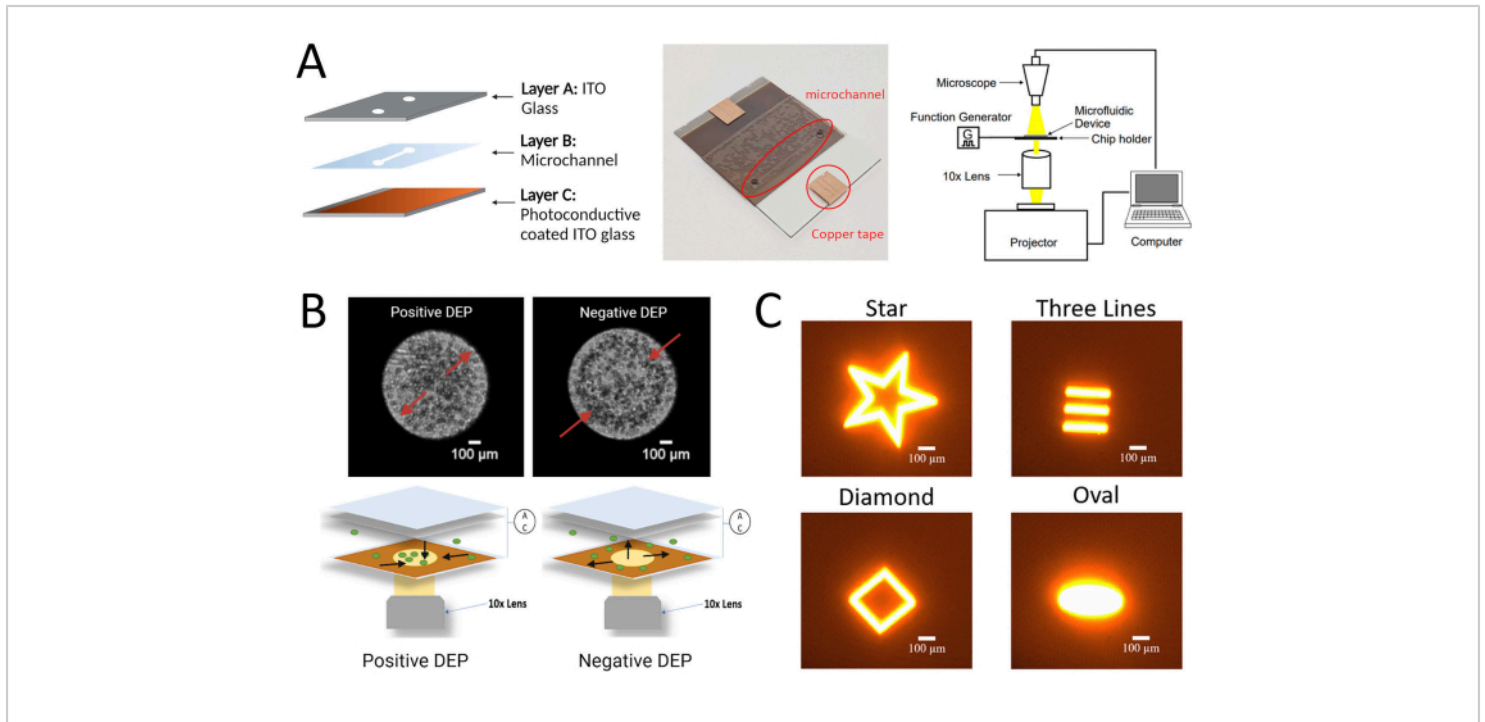


Figure 1: Experimental setup for the LiDEP protocol described here for hMSCs. (A) Schematic and real image of the LiDEP chip with the photoconductive layer and the experimental set-up. **(B)** Representative images of positive and negative DEP responses of cells in the 3DEP analyzer (using conventional DEP electrodes, top) and schematic representation of positive and negative DEP responses of cells using LiDEP (using light projections as virtual electrodes, bottom). **(C)** Examples of different shapes that can be projected onto the device as virtual electrodes. Figure created with BioRender.com. [Please click here to view a larger version of this figure.](#)

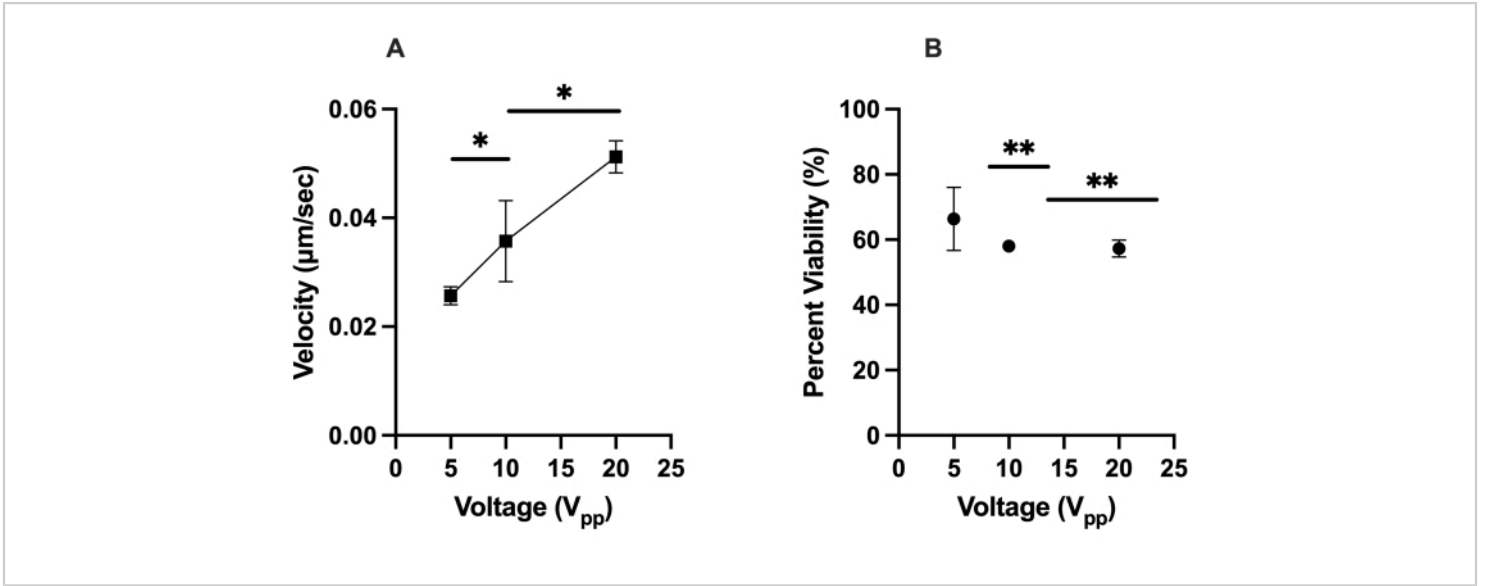


Figure 2: Characterization of the DEP responses (velocity) of hMSCs and their viability under the given conditions.

(A) The measured velocities of the positive DEP responses of hMSCs to 5 V_{pp} , 10 V_{pp} , and 20 V_{pp} . The hMSCs moved at 0.051 $\mu\text{m/s}$ at 20 V_{pp} , 0.036 $\mu\text{m/s}$ at 10 V_{pp} , and 0.025 $\mu\text{m/s}$ at 5 V_{pp} . (B) The viability of the hMSCs after experiencing the positive DEP force generated with virtual electrodes. The viability was 57%, 58%, and 66% for 20 V_{pp} , 10 V_{pp} , and 5 V_{pp} , respectively. Error bars represent the standard deviation (SD). Statistical analysis completed on pooled data sets using t-tests ($*p < 0.05$ and $**p < 0.01$). [Please click here to view a larger version of this figure.](#)

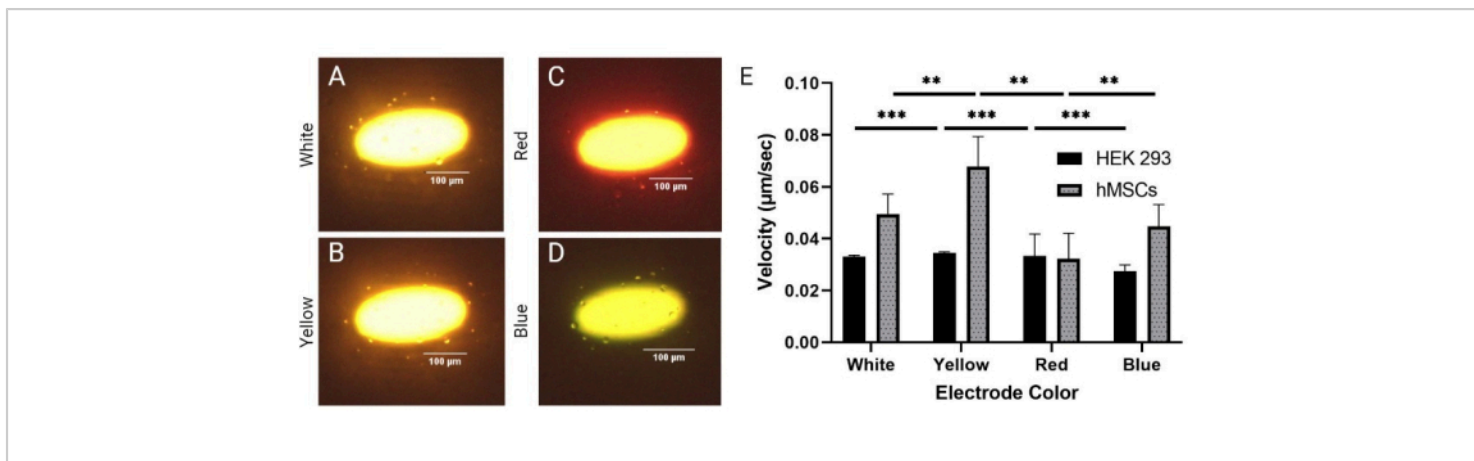


Figure 3: Comparing the DEP responses between homogenous (HEK 293) and heterogenous (hMSCs) cell lines. Positive DEP response of hMSCs cells to (A) white, (B) yellow, (C) red, and (D) blue electrodes at 20 V_{pp} and 30 kHz. (E) Velocity responses of HEK 293 cells and hMSCs to the different colored electrodes. The HEK 293 cells exhibited the highest velocities with the yellow and red electrodes at 0.035 $\mu\text{m/s}$ and 0.033 $\mu\text{m/s}$, respectively. The HEK 293 cells exhibited the lowest velocity with the blue electrodes at 0.027 $\mu\text{m/s}$. The hMSCs exhibited the highest velocities with the yellow and white electrodes at 0.068 $\mu\text{m/s}$ and 0.049 $\mu\text{m/s}$, respectively. The hMSCs experienced the lowest velocity with the red electrodes at 0.039 $\mu\text{m/s}$. The error bars represent the SD. Statistical analysis completed on pooled data sets using t-tests (* $p < 0.05$, ** $p < 0.01$, and *** $p < 0.001$). [Please click here to view a larger version of this figure.](#)

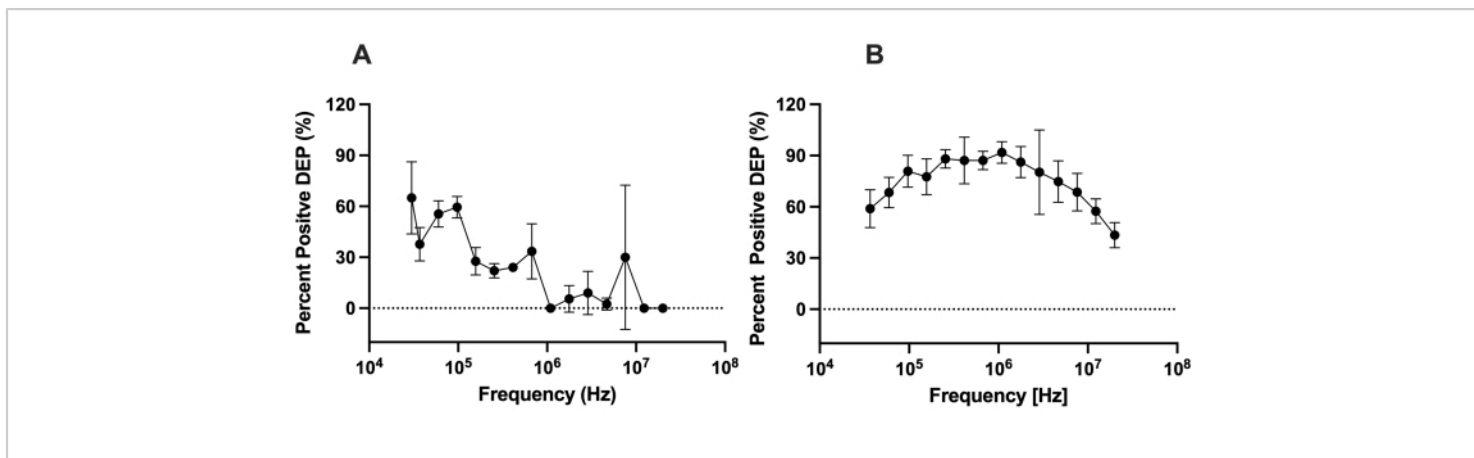


Figure 4: Comparing the DEP responses of hMSCs using LiDEP and 3DEP. The DEP responses of hMSCs measured with (A) LiDEP and (B) the 3DEP analyzer at 10 V_{pp}. With LiDEP, there was a decay in the positive DEP response of the hMSCs from 30 kHz to 20 MHz. From the 3DEP analyzer, the cells increased in positive DEP from 37 kHz to 255 kHz and decreased in positive DEP from 1,772 kHz to 20 MHz. Error bars represent the SD. [Please click here to view a larger version of this figure.](#)

Supplementary Figure 1: Representative images of the LiDEP setup used for the experiments in this protocol.

Zoomed-in picture of the LiDEP system showing the integration of the projector. Light travels from the source (projector) through a 10x objective lens onto the microchannel of the LiDEP chip. The 10x objective sits on top of the projector lens. Each component is numbered in the pictures and listed on the side. [Please click here to download this File.](#)

Supplementary Video 1: Representative video of hMSCs responding to the white, yellow, red, and blue virtual electrodes.

The cells are visualized as experiencing positive DEP (moving toward the virtual electrode), experiencing negative DEP (moving away from the virtual electrode), stationary and rotating, or unresponsive to the electric field. The hMSCs were tested at 37 kHz and 20 V_{pp}, and the video was sped up 20x. [Please click here to download this File.](#)

Discussion

Examining the heterogeneity of hMSCs is important for their advancement in therapeutics. This work provides a first step for using LiDEP as an analytical tool for the assessment of hMSCs. We examined the voltage dependency of the positive DEP response of cells in LiDEP by quantifying the velocity. It is expected that higher voltages should produce stronger positive DEP force, and we observed this pattern with the velocities measured. The 10 V_{pp} and 20 V_{pp} voltages were sufficient for the manipulation of hMSCs using LiDEP. Lower voltages (i.e., 5 V_{pp}) resulted in slower cell responses; while not optimal for hMSCs, this could be advantageous for other cell types. There was a voltage-dependent decrease in the viability of the hMSCs of approximately 9%. This slightly differs from the previous literature^{6,12,28,29}, in which the use of traditional DEP and LiDEP in the examination of biological cells did not decrease the cell viability. However, the experimental objective in each study varied. Glasser and Fuhr

monitored the growth of adherent L929 mouse fibroblasts on metal electrodes in cell culture medium²⁸. Conversely, Lu et al. examined the viability of neural stem cells exposed to AC electric fields for different periods of time¹². Adams et al. characterized the dielectric properties of hMSCs with metal electrodes¹², and Li et al. manipulated leukemia cells with LiDEP²⁹. The difference between these studies and ours was the use of BSA, which may be the cause of the decrease in viability we observed. However, the lower overall viability may also be due to the exposure time (2 min 30 s) used in the protocol established here. This time was chosen to provide enough time to visualize cell manipulation during exposure to the nonuniform AC electric field.

The methods of cell characterization were tested *via* the electrode color to determine the capabilities and limitations of our LiDEP system built as described in the protocol. In this specific protocol, the electrode color can be controlled based on the color of the shape being projected through a graphic editor file. We used four colors: white, yellow, red, and blue. From the power output readings for each color, the projected yellow (#FFFF00) and white (#FFFFFF) electrodes were measured to have higher intensities, which was the basis of why these colors were more favorable to use in the subsequent experiments. Additionally, because of the established light intensity dependence of photoconductive materials^{30,31}, the results suggest that the performance of LiDEP devices relies on photoconductive A:Si and can be tuned by the choice of the projected electrode color. A combination of positive and negative DEP responses of hMSCs was also observed using LiDEP, which is like the phenomenon seen in traditional DEP methods. With each electrode color, the hMSCs experienced negative DEP force, positive DEP force, and cell rotation, indicating that the cell sample was heterogeneous at a single frequency

(**Supplementary Video 1**). This agrees with the findings of Adams et al.⁶ that hMSCs exhibit both negative and positive DEP behavior at a single frequency. These conditions (electrode color, electrode shape, and photoconductive material) may provide additional parameters for detecting the level of heterogeneity in hMSC samples.

Lastly, the results of the LiDEP assessment were compared to results from the 3DEP analyzer as a benchmark of hMSC DEP behavior. A difference in the frequency range of the positive DEP response of hMSCs was observed, but the trends in the data collected *via* LiDEP and the 3DEP analyzer were similar overall (i.e., the positive DEP response decreased with increased frequency). When the AC electric field was supplied to the LiDEP chip and light was projected onto it, the conductance in the area within the light projection dropped, creating a nonuniform electric field. Therefore, the characteristics of the light source (i.e., intensity and wavelength) influence the expected response of the cells within the LiDEP chip, as seen from the results of the voltage and electrode color variation tests. Other parameters that can be modified are the material of the photoconductive layer and the conductivity of the DEP buffer solution. As such, the conditions used to evaluate the DEP behavior of cells must be evaluated based on the setup of the LiDEP system. Conversely, for the 3DEP analyzer, or other methods that use metal electrodes to apply the DEP force, the electrode characteristics are constant and cannot be varied instantly to adapt to what is needed for the cells under investigation. This variation of the positive DEP behavior could be beneficial for future research into the characterization of different cell types within hMSC samples, single-cell analysis, or cell sorting. In addition, as the cells move farther away from the virtual electrodes, the AC electric field becomes weaker. However, with the 3DEP analyzer, or other traditional DEP

modes that use metal electrodes, a larger electric field region can be applied, which allows for more cells to be manipulated. Therefore, fewer cells per LiDEP experiment experienced the effects of the AC electric field within the microchannel of the LiDEP chip. Further discrepancies may be caused by changes in device performance over time (i.e., 2 h or 3 h), which is still being investigated. The constant flow of water, ethanol, and DEP buffer solution could break down the surface of the microchannel layer (i.e., the photoconductive material) and needs to be considered. The device performance over time for cell characterization also needs to be considered for the extended use of one LiDEP chip. Modifications to the experimental parameters in real-time only took a few seconds to minutes. The electrode color and geometries were adjusted instantly using settings within the graphic editor software.

In summary, this paper demonstrates the capabilities of LiDEP to manipulate and characterize a cell line with heterogeneous cell populations such as hMSCs. Using this setup and the described protocol, we were able to achieve the successful characterization of hMSCs under the conditions of 20 V_{pp} and projected virtual yellow electrodes. Future studies should focus on adjusting the exposure time of the hMSCs to the AC electric field created *via* LiDEP, increasing the light intensity of the virtual electrodes, and assessing different sources of hMSCs (or other stem cell populations) to develop a LiDEP catalog of the electrical signatures of heterogeneous stem cell populations.

Disclosures

The authors report no conflicts of interest.

Acknowledgments

This work was supported by the National Science Foundation CAREER award (2048221) *via* CBET. We would like to acknowledge Mo Kebaili from the UCI's Integrated Nanosystems Research Facility (INRF). Additionally, we would like to thank Dr. Devin Keck for assisting with the development of the LiDEP system.

References

1. Mahla, S. R. Stem cells applications in regenerative medicine and disease therapeutics. *International Journal of Cell Biology*. **2016**, 6940283 (2016).
2. Bhansali, A. et al. Efficacy of autologous bone marrow-derived stem cell transplantation in patients with type 2 diabetes mellitus. *Stem Cells and Development*. **18** (10), 1407-1416 (2009).
3. Bouchlaka, M. N. et al. Human mesenchymal stem cell-educated macrophages are a distinct high IL-6-producing subset that confer protection in graft-versus-host-disease and radiation injury models. *Biology of Blood and Marrow Transplantation*. **23** (6), 897-905 (2017).
4. Alfaifi, M., Eom, Y. W., Newsome, P. N., Baik, S. K. Mesenchymal stromal cell therapy for liver diseases. *Journal of Hepatology*. **68** (6), 1272-1285 (2018).
5. Oswald, J. et al. Mesenchymal stem cells can be differentiated into endothelial cells in vitro. *Stem Cells*. **22** (3), 377-384 (2004).
6. Sakaguchi, Y., Sekiya, I., Yagishita, K., & Muneta, T. Comparison of human stem cells derived from various mesenchymal tissues: superiority of synovium as a cell source. *Arthritis and rheumatism*. **52**(8), 2521-2529 (2005).

7. Poirier, J. T. Chapter 5 - Genetic profiling of tumors in PDX models. In *Patient Derived Tumor Xenograft Models: Promise, Potential and Practice.*, edited by Uthamanthil, R., Tinkey, P., 149-159. Academic Press. Cambridge, MA (2017).
8. Sino Biological. *Fluorescence-activated cell sorting (FACS)*. at <<https://www.sinobiological.com/category/fcm-facs-facs>>. (2023).
9. González-González, M., Vázquez-Villegas, P., García-Salinas, C., Rito-Palomares, M. Current strategies and challenges for the purification of Stem Cells. *Journal of Chemical Technology and Biotechnology*. **87** (1), 2-10 (2011).
10. Flanagan, L. A. et al. Unique dielectric properties distinguish stem cells and their differentiated progeny. *Stem Cells*. **23** (3), 656-665 (2007).
11. Vykoukal, J., Vykoukal, D. M., Freyberg, S., Alt, E. U., Gascoyne, P. R. C. Enrichment of putative stem cells from adipose tissue using dielectrophoretic field-flow fractionation. *Lab on a Chip*. **8** (8), 1386-1393 (2008).
12. Adams, T. N. G., Turner, P. A., Janorkar, A. V., Zhao, F., & Minerick, A. R. Characterizing the dielectric properties of human mesenchymal stem cells and the effects of charged elastin-like polypeptide copolymer treatment. *Biomicrofluidics*. **8**(5), 054109 (2014).
13. Wu, H. W., Lin, C. C., Lee, G. B. Stem cells in microfluidics. *Biomicrofluidics*. **5** (1), 013401 (2011).
14. Adams, T. N. G. et al. Label-free enrichment of fate-biased human neural stem and progenitor cells. *Biosensors and Bioelectronics*. **152**, 111982 (2020).
15. Zhao, K., Larasati, Duncker, B. P., Li, D. Continuous cell characterization and separation by microfluidic alternating current dielectrophoresis. *Analytical Chemistry*. **91** (9), 6304-6314 (2019).
16. Song, H. et al. Continuous-flow sorting of stem cells and differentiation products based on dielectrophoresis. *Lab on a Chip*. **15**, 1320-1328 (2015).
17. Khoshmanesh, K., Nahavandi, S., Baratchi, S., Mitchell, A., Kalantar-Zadeh, K. Dielectrophoretic platforms for bio-microfluidic systems. *Biosensors and Bioelectronics*. **26** (5), 1800-1814 (2010).
18. Hoettges, K. F. et al. Ten-second electrophysiology: Evaluation of the 3DEP platform for high-speed, high-accuracy cell analysis. *Scientific Reports*. **9**, 19153 (2019).
19. Hubner, Y., Hoettges, K. F., Kass, G. E. N., Ogin, S. L., Hughes, M. P. Parallel measurements of drug actions on Erythrocytes by dielectrophoresis, using a three-dimensional electrode design. *IEE Proceedings - Nanobiotechnology*. **152** (4), 150-154 (2005).
20. Hoettges, K. F. et al. Dielectrophoresis-activated multiwell plate for label-free high-throughput drug assessment. *Analytical Chemistry*. **80** (9), 2063-2068 (2008).
21. Mulhall, H. J. et al. Cancer, pre-cancer and normal oral cells distinguished by dielectrophoresis. *Analytical and Bioanalytical Chemistry*. **401** (8), 2455-2463 (2011).
22. Liao, C.-J. et al. An optically induced dielectrophoresis (ODEP)-based microfluidic system for the isolation of high-purity CD45neg/EPCAMNEG cells from the blood samples of cancer patients-Demonstration and initial exploration of the clinical significance of these cells. *Micromachines*. **9** (11), 563 (2018).

23. McGrath, J. S. et al. Electrophysiology-based stratification of pancreatic tumorigenicity by label-free single-cell impedance cytometry. *Analytica Chimica Acta*. **1101**, 90-98 (2019).
24. Chiu, T. K. et al. Optically-induced-dielectrophoresis (ODEP)-based cell manipulation in a microfluidic system for high-purity isolation of integral circulating tumor cell (CTC) clusters based on their size characteristics. *Sensors and Actuators, B: Chemical*. **258**, 1161-1173 (2018).
25. Medjdoub, M., Courant, J. L., Maher, H., Post, G. Inductively coupled plasma - plasma enhanced chemical vapor deposition silicon nitride for passivation of InP based high electron mobility transistors (HEMTs). *Material Science and Engineering: B*. **80** (1-3), 252-256 (2001).
26. ATCC. *Umbilical cord-derived mesenchymal stem cells; Normal, human*. <<https://www.atcc.org/products/pcs-500-010>>. (2023).
27. ATCC. *293 [HEK-293]*. <<https://www.atcc.org/products/crl-1573>>. (2023).
28. Glasser, H., Fuhr, G. Cultivation of cells under strong ac-electric field-differentiation between heating and trans-membrane potential effects. *Bioelectrochemistry and Bioenergetics*. **47** (2), 301-310 (1998).
29. Li, B. et al. Implementation of flexible virtual microchannels based on optically induced dielectrophoresis. *Nanotechnology*. **33**, 295102 (2022).
30. Schellenberg, J. J., Kao, K. C. On the relationship between photoconductivity and light intensity in solids. *Journal of Physics D: Applied Physics*. **21**, 1764-1768 (1988).
31. Aoyagi, Y., Masuda, K., Namba, S. Explanation of light-intensity dependence of photoconductivity in zinc phthalocyanine. *Journal of Applied Physics*. **43**, 249-251 (1972).